Scanning Electron Microscopy

Volume 1985
Number 1 *1985*

Article 11

11-7-1984

Characterization of Carbonaceous Materials by Correlated Electron and Optical Microscopy and Raman Microspectroscopy

C. Beny-Bassez
GIS BRGM-CNRS

J. N. Rouzaud
Laboratoire Marcel Mathieu, CNRS

Follow this and additional works at: https://digitalcommons.usu.edu/electron

 Part of the Biology Commons

Recommended Citation

Beny-Bassez, C. and Rouzaud, J. N. (1984) "Characterization of Carbonaceous Materials by Correlated Electron and Optical Microscopy and Raman Microspectroscopy," *Scanning Electron Microscopy*: Vol. 1985 : No. 1 , Article 11.
Available at: https://digitalcommons.usu.edu/electron/vol1985/iss1/11

This Article is brought to you for free and open access by the Western Dairy Center at DigitalCommons@USU. It has been accepted for inclusion in Scanning Electron Microscopy by an authorized administrator of DigitalCommons@USU. For more information, please contact digitalcommons@usu.edu.

UtahStateUniversity
MERRILL-CAZIER LIBRARY

SCANNING ELECTRON MICROSCOPY/1985/I (Pages 119-132)
SEM Inc., AMF O'Hare (Chicago), IL 60666 USA
0586-5581/85$1.00+.05

CHARACTERIZATION OF CARBONACEOUS MATERIALS BY CORRELATED ELECTRON AND OPTICAL MICROSCOPY AND RAMAN MICROSPECTROSCOPY

C. BENY-BASSEZ[*] and J.N. ROUZAUD[**]

[*]GIS BRGM-CNRS, 1A rue de la Férollerie - 45045 ORLEANS CEDEX, FRANCE
[**]Laboratoire Marcel Mathieu, CNRS, UER Sciences - 45046 ORLEANS CEDEX, FRANCE

(Paper received April 3 1984, Completed manuscript received November 7 1984)

Abstract

Carbonaceous materials differ according to their chemical composition (types of heteroatoms), their structure and their microtexture. So, it is interesting to find methods for characterizing them. We choose to correlate data from Raman microspectroscopy, optical microscopy and transmission electron microscopy. First, we use both graphitizable or non-graphitizable reference carbon series of simple chemical composition in order to follow the structural transformation of the carbonaceous materials according to the evolution of these data throughout heat-treatment of these samples. Then, the coals of different ranks are studied.

The Raman results are correlated with those from electron microscopy, particularly by plotting, for the graphitizable series, the diameter of the aromatic layers L_a (determined from lattice fringes and 11 dark-field) versus the specific surface of the Raman band characteristic of the defects centered at about 1350 cm^{-1} (ratio between surfaces of this band and the whole spectrum). For the coals, the half-maximum width of the band at about 1600 cm^{-1} has been plotted versus the reflectance.

We conclude that the evolution of carbonaceous materials, throughout heat-treatments or natural processes, is possible only because different types of defects are progressively removed. These defects are heteroatoms, tetrahedral carbons, isolated and crosswise basic structural units or BSU (one, two or three stacked in parallel polyaromatic structures, less than 10 Å in size) and defects in aromatic layers. The elimination of these defects permits the rearrangement of the BSUs and the establishment of an organization which can possibly reach the triperiodic order according to the series.

KEY WORDS: Carbonaceous materials, Raman microprobe, high resolution electron microscopy, optical microscopy.

*Address for correspondence:
C. Beny-Bassez
GIS BRGM-CNRS, 1A rue de la Férollerie
45045 - Orléans Cedex, France
Phone No. (011) 33-38632142

Introduction

The term "carbonaceous materials" designates all substances of which the major component is carbon. These materials can be either rich in heteroatoms such as hydrogen , oxygen, nitrogen, sulfur, etc (for instance coals contain 77 to 95% carbon, or nearly pure carbons (carbon fibers, cokes with 91 to 99% carbon), or crystallized or amorphous pure carbons (natural or synthetic graphite or glassy carbon respectively). Carbonaceous materials are either natural for example coals, parent rocks of petroleum, or synthetic such as cokes, pitches, pyrocarbons, composite materials, etc. Therefore, the chemical composition, the structure and the microtexture can be very different according to the carbonaceous materials.

The characterization of these substances is very important especially to differentiate them and determine their behavior during heat-treatments and from here, to predict their physico-chemical properties. Such information is of great interest for understanding the mechanisms of carbonization either through natural processes in the sediments submitted to the geothermal gradient (coalification, i.e. geological process) or in a furnace (industrial process). Therefore, different carbonaceous materials with an increasing carbon content were obtained from different organic precursors.

Different techniques are used to study carbonaceous materials such as elemental analysis (10,11,18,34,39,45), X-ray diffraction (12,14, 15,22,45,46), infrared and Raman spectroscopy (36-38; 3,19,20,25,26,39,41,44,47,48), optical (1,2,13,16,21,35,39,41,43,45,46) and electron (4,5,6,17,24,27-33,39-41) microscopy. However, the degree of coalification (or rank) of coals is, in general, characterized by their reflectance. It is conventionally measured on vitrinite (1, 43), the predominant microscopically recognizable constituent of most coals. The reflectance of vitrinite increases progressively with the rank. Its value depends on chemical composition, structure and microtexture. Since these three parameters vary together during coalification, the same measured reflectance can correspond to different coals (39,40). So, the reflectance data have to be complemented by results obtained by

other techniques, for example elemental analyses for the chemical composition, transmission electron microscopy and microRaman spectroscopy for determining the structure and the microtexture.

In order to minimize the influence of the chemical composition parameter and to try to establish comparisons with results from different techniques, it has seemed advisable to study, at first, carbons of simple chemical composition. So, we chose series of carbons either graphitizable such as carbon films, heat-treated from room temperature to 2700°C, and anthracene semi-coke, heat-treated from 450 to 2900°C, or non-graphitizable such as saccharose semi-coke, heat-treated from 400 to 3000°C. Then, we have worked on more complex carbonaceous materials such as coals of different ranks.

Until now, very few Raman studies have been performed on coherent series of carbons (20). On the contrary; in this work, the results obtained by Raman microspectroscopy, optical and electron microscopy enable us to propose a process of evolution of the microtexture and structure during the carbonization -natural or artificial- and graphitization. Some results obtained on carbon films from the same three combined techniques have been previously published in Thin Solid Films (41). In the present work, complementary data on films and new results on other carbon series (anthracene - cokes and saccharose - cokes) are given and compared for discussion. All carbonaceous materials contain similar basic structural units or BSU, (one, two or three stacked in parallel polyaromatic structures, less than 10 Å in size). These units are, first, distributed at random, then at a temperature about 500°C, they are oriented in parallel in areas the size of which depends on the chemical composition of the material. Oxygen-free materials (anthracene-cokes, for instance) show large molecular orientations (few micrometers). On the contrary, oxygen-rich materials (saccharose-cokes, for instance) exhibit only small molecular orientations ($\sim$ 50 Å). It is the size of these molecular orientations which determines the graphitizability of the material: the first ones are graphitizable, the second ones remain biperiodical even at 3000°C. According to the chemical nature of carbonaceous materials, all intermediates exist between these two microtextural poles.

Sampling

Carbon Films

The carbon films were prepared at room temperature in a 10^{-5} Torr vacuum by condensing onto a NaCl substrate a carbon vapor, obtained by fast evaporation (few seconds at the most) of two graphite electrodes presenting a poor electric contact. After the dissolution of the substrate, small portions of carbon films were picked up on carbon grids. The films obtained are supple and fragile and tend to fold during manipulations. The films on these grids were heat-treated under argon flow inside a furnace (heating rate, 20°/mn; residence time, 15mn). Samples were prepared by 100°C steps, which became 30°C steps when the properties of the samples varied too quickly. The thickness of the films depends on the evaporation duration and the distance between the electrodes.

Two series of films were studied: thick films (thickness of about 500 Å) and thin films (thickness of about 150 Å).

For electron microscopy, the films were studied directly on the carbon grids. For optical microscopy and Raman microspectroscopy, these films were transferred onto glass slides. Polyaromatic structures and then aromatic layers of the films are oriented parallel to the film plane (17) and consequently parallel to the glass slide plane. Thus, in the flat portions of the films, aromatic layers are oriented normally to the incident beam.

Anthracene-Cokes

The original anthracene semi-coke, which contains only one type of heteroatoms (hydrogen), was obtained by pyrolysis of anthracene ($C_{14}H_{10}$) at 450°C under about 20 bars. From this semi-coke, the anthracene-cokes were obtained by pyrolysis under argon flow from 500 to 2900°C by 100°C steps.

For electron microscopy, the anthracene-cokes were ground and gave lamellae laying preferentially flat on the grids. Polished sections were used to measure the reflectance and to obtain the Raman spectrum.

Saccharose-Cokes

The original saccharose semi-coke, which contains oxygen and hydrogen as heteroatoms, was obtained by pyrolysis of saccharose ($C_{12}H_{22}O_{11}$) at 400°C under atmospheric pressure. From this semi-coke, the saccharose-cokes were obtained by pyrolysis until 3000°C by 100°C steps.

The preparation of the samples for the studies by the different techniques was the same as for the anthracene-cokes.

Coals

The coals studied are natural samples from different geological and/or geographical origins. This series shows various degrees of coalification from volatile bituminous coals (mean reflectance measured in oil about 0.75%) to anthracites (mean reflectance in oil up to 5%). They contain different types of heteroatoms, progressively released as the rank increases.

The preparation of the coals for the studies was the same as for the saccharose-cokes.

Description of the Techniques

Optical Microscopy (monochromatic light: λ=546nm)

For bulk materials (anthracene-cokes, saccharose-cokes and coals), the real refractive index and the extinction coefficient were calculated from reflectance values determined in two different media (air and oil) with the help of Fresnel's equation. We saw that errors on reflectance measurements affect mainly calculations on the refractive index. So, variations of the extinction coefficient were preferred.

Transmission Electron Microscopy (TEM)

The different TEM modes (5,41) were applied to the carbonaceous materials (002, 10 and 11 dark-field; 002 lattice fringes; Selected Area Electron Diffraction (SAED). The 002 dark-field

and lattice fringe images permit the direct visualization and the measurement of the planar polyaromatic structures which are present in the studied sample. The optical diffraction patterns of lattice fringe images (visualization of the aromatic layers seen edge-on) and densitometric recordings allow one to measure the average twist angle β between two adjacent aromatic layers and the variation ΔD in the interfringe spacing. Throughout the heat-treatment, the number N of parallel aromatic layers in the BSU is measured by lattice fringe technique and the diameter L_a of this unit is determined by 11 dark-field. The graphitization itself is followed by means of SAED patterns by progressive modulation of hk bands (biperiodic order) into hkℓ reflections (triperiodic order).

Raman Spectroscopy

The light scattered by a sample illuminated by a monochromatic light beam (ν_0) is polychromatic with a strong component at the same frequency ν_0 (Rayleigh scattering) and several weak components at frequencies $\nu_0 \pm \nu_i$. The Raman effect corresponds to these changes of frequency, which are characteristic of the polyatomic groups present in the illuminated sample.

Laser light sources have permitted important improvements of Raman techniques as well as the design of Raman microprobes such as the Molecular Optical Laser Examiner (MOLE) microprobe (7,9). The most recent developments in the optical and detection fields have led to the creation of Raman multichannel microprobes (8,23,42).

The Raman microspectroscopic studies, presented below, have been obtained at room temperature, after cooling of the heat-treated samples. They have been performed on a MOLE microprobe. In a few words, the principle is the following: a laser beam falls at normal incidence and is focused by means of an optical microscope and one of its objectives, on a small area of the carbonaceous material, in this case (few μm^2, i.e. about 10^{-13} g for the thin carbon films). The light scattered by the sample is collected by the same objective and analyzed with the help of a double concave holographic grating spectrometer followed by a photomultiplier, a photon counter and a chart recorder.

In the case of some carbonaceous materials (such as low-rank coals, cokes heat-treated below 800-1000°C) a local degradation of samples due to heating by a too powerful laser beam has been observed (dark area at the laser beam impact, shift of Raman spectrum base line). To avoid these degradations, some precautions must be taken. So, the general conditions to record the Raman spectra presented below have been chosen 40 to 250mW power of the 514.5nm radiation at the exit of the laser corresponding to a power of 0.4 to 2.5mW at the sample, 300µm slit widths, x100 or x160 objective, 0.7 or 1.5s counting time.

The first-order Raman spectrum of pure graphite (26,44) has a well-known sharp band at 1580 cm^{-1} which corresponds to the E_{2g} vibration mode (carbon-carbon vibration in the aromatic layers). The Raman spectra of carbonaceous materials (3,20,25,26,39,41,48) show two bands, one at about 1580-1610 cm^{-1} and the other at about 1350-1380 cm^{-1}. The existences, half-maximum widths, surfaces and wavenumbers of each band are parameters which depend on the organization and the defects (heteroatoms, defects in aromatic layers or between aromatic layers and probably also tetrahedral carbons) in the sample. The variations of these parameters, versus the temperature, could permit to follow the evolution of the sample.

The maximum band frequencies, half-maximum widths, specific surface of defect band (ratio between area of defect band and whole spectrum area) and ratio between areas of bands at about 1580 and 1350 cm^{-1} are determined from graphically smoothed spectra then decomposed manually or by computer.

Raman Results

Graphitizable Carbonaceous Materials

The crude Raman spectra of the reference series (anthracene-cokes, thick and thin carbon films) are shown in Figures 1, 2 and 3. Throughout heat-treatments, the general evolution of the Raman spectra is the same for each of the three different series. The two bands at about 1350 and 1580 cm^{-1}, broad at room temperature, become sharper more or less rapidly and more or less gradually according to the temperature range and the carbon series. Finally, there remains only one band at 1580 cm^{-1}, frequency of the E_{2g} vibration mode in the plane of aromatic layers of graphite.

The variations of the Raman parameters versus temperature are also roughly the same for the various series. However, they permit to note more precisely the evolution differences among the three types of carbonaceous materials.

Half-Maximum Widths: Figures 4 and 5 exhibit similar variations for the three series of materials. Figure 4 shows that for the defect band (1350 cm^{-1}), the half-width l_{1350} decreases from about 250 to 50 cm^{-1} before it disappears. This decrease is rapid until 1500°C and slightly slower until its disappearance at a temperature between 2500-2900°C according to the series. l_{1350} is only a bit sharper for the anthracene-cokes than for the carbon films. On the other hand, Figure 5 shows great differences of the half-width of the 1580 cm^{-1} band, l_{1580}, between the anthracene-cokes and the carbon films. Below 1400°C, l_{1580} of carbon films is nearly twice that of anthracene-cokes. That suggests a perturbation which exists only in the carbon films. Above 1400°C, the thick films and the anthracene-cokes have nearly the same l_{1580}, whereas the thin films have a more pronounced one until 2100°C.

Frequency Shifts of the Band Maxima: The differences between the three series are significant only for the defect band (Figures 6a and 6b). The anthracene-cokes exhibit a maximum frequency always at 1350 cm^{-1} (Figure 6b), while for the carbon films this maximum shifts towards higher frequencies and can reach 1400 cm^{-1} between 1300 and 1400°C. Moreover there is a non-monotonic behaviour at about 1340-1375°C in the case of the thick films (for the thin ones, the number of

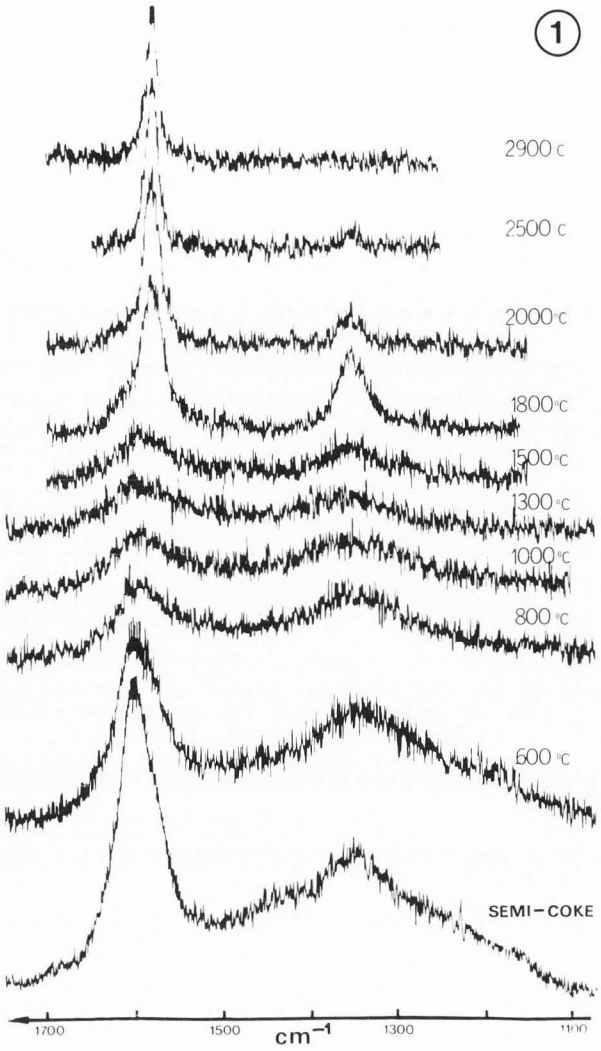

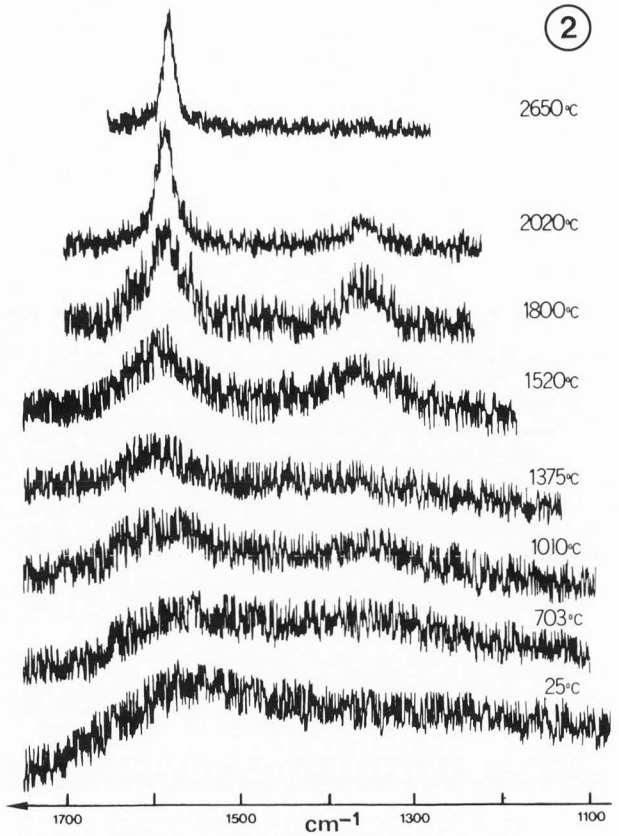

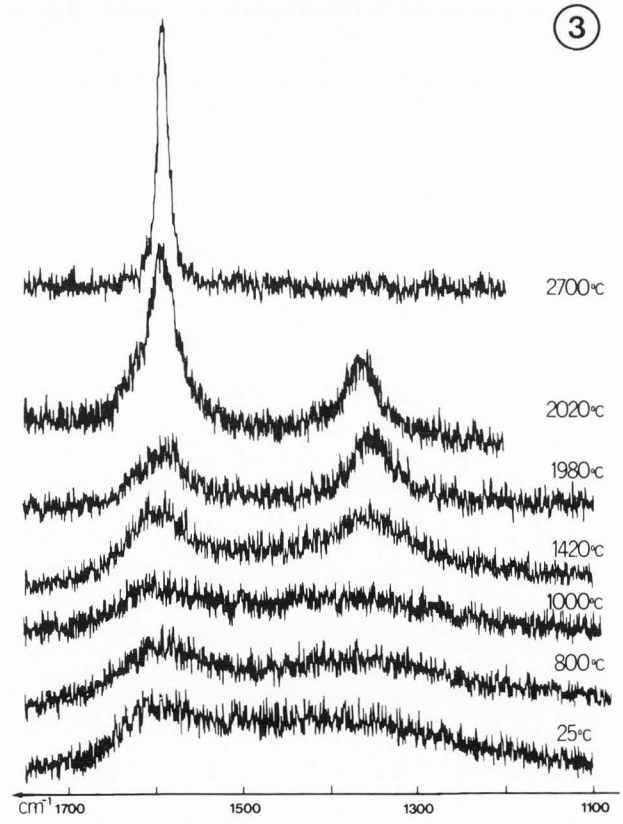

Figure 1 - Raman spectra of anthracene-cokes heat-treated at different temperatures.

Figure 2 - Raman spectra of thick carbon films heat-treated at different temperatures.

Figure 3 - Raman spectra of thin carbon films heat-treated at different temperatures.

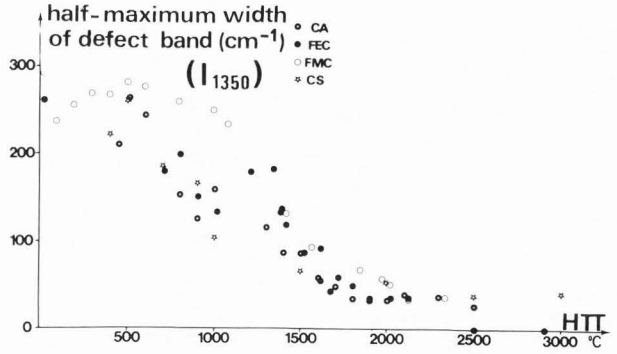

Figure 4 - Half-maximum width of band at 1350 cm^{-1} (I_{1350}) versus heat-treatment temperature (HTT) (CA: anthracene-cokes; FEC: thick carbon films; FMC: thin carbon films; CS: saccharose-cokes).

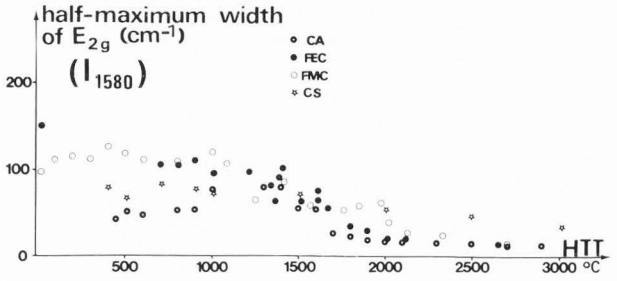

Figure 5 - Half-maximum width of band at 1580 cm^{-1} (I_{1580}) versus HTT (anthracene- and saccharose-cokes, carbon films).

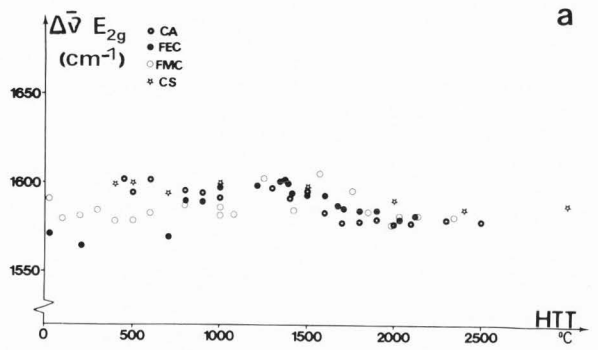

Figure 6a - E_{2g} band wavenumber ($\Delta\bar{\nu}E_{2g}$) versus HTT.

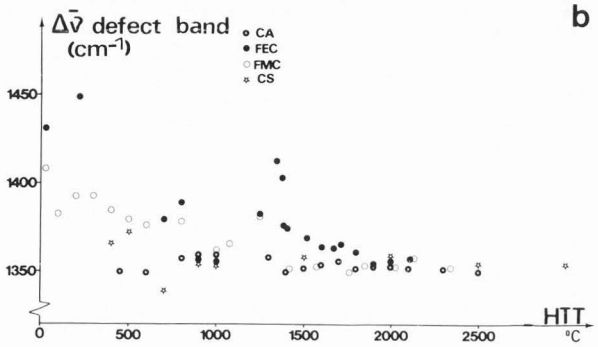

Figure 6b - Defect band wavenumber versus HTT.

heat-treated samples was too small for showing clearly the same behaviour, but this one could exist in this temperature range).

Surface of the Band at 1350 cm^{-1} (S_{1350}): Figures 7 and 8 can be compared and indicate that the variations are roughly similar for the three series. The band decreases and disappears at about 2500°C for the thick carbon films, 2700°C for the thin carbon films and 2900°C for the anthracene-cokes.

Decomposition of the Defect Band: The band at about 1350 cm^{-1} is attributed to defects present in the aromatic structure. It is worth noting that in the anthracene-cokes, the bonds are all of the same type and the defect band frequency is constant (Figure 6b), whereas for the carbon films there is a frequency shift of the defect band and a most pronounced width of the band at about 1580 cm^{-1} (Figure 5). This suggests, therefore, the existence of supplementary types of defects in the carbon films. This is the reason why the spectra of the carbon films (principally, spectra of the thick carbon films for which the temperatures of heat-treatments were more closely spaced) have been decomposed by computer into three bands, one at about 1580 cm^{-1} always attributed to the aromatic carbons and two at about 1350 and 1500 cm^{-1} attributed to the defects. Figures 9 and 10 show the variations of the specific surfaces of these two last bands versus the temperature for the thick carbon films. These variations are antisymmetric. The shape of the curve related to the 1500 cm^{-1} band is similar to that related to the variation ΔD in the interfringe spacing (Figure 11), whereas the curve related to the 1350 cm^{-1} band is similar to that related to the average angle β between two aromatic layers (Figure 12). The same oscillations are observed in the 1300-1500°C range in electron microscopy and in Raman microspectroscopy. The band at about 1500 cm^{-1} disappears at 1670°C. It is at this temperature that the cross-wise BSUs disappear permitting the increasing of the layer diameter, L_a, (see below). So, the band at 1500 cm^{-1} or the part, which remains after the decomposition in two symmetric bands at about 1350 and 1580 cm^{-1}, has been attributed to the defects outside the plane of the aromatic layers such as tetrahedral carbons. The band symmetric at about 1350 cm^{-1} is attributed to the defects in the plane of the aromatic layers; it decreases as the stiffening of planes increases (β decreases).

Non-Graphitizable Carbonaceous Materials: Saccharose-Cokes.

Whatever the temperature, the Raman spectra exhibit two bands (Figure 13) at about 1350 and 1580 cm^{-1}. The specific surface of the Raman defect band S_{1350} (Figure 7) and the ratio S_{1350}/S_{1580} (Figure 8) are approximately constant, the defects are not eliminated throughout the heat-treatment. On the other hand, the comparison

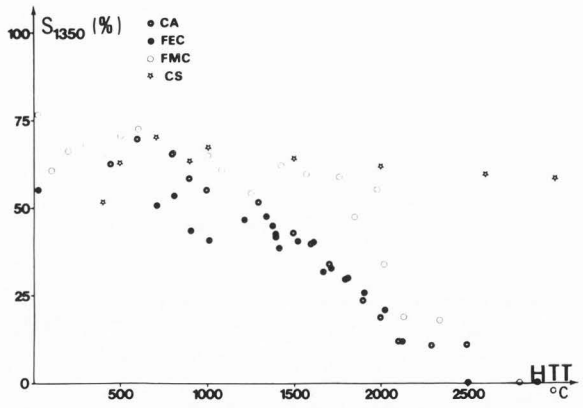

Figure 7 - Specific surface of the Raman defect band (S_{1350}) versus HTT (anthracene- and saccharose-cokes, carbon films).

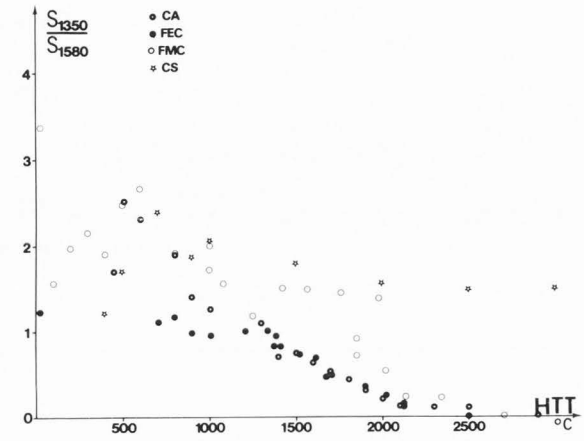

Figure 8 - Ratio between S_{1350} and S_{1580} versus HTT (anthracene-cokes and carbon films).

of the data obtained for the two coke series (Figures 4,5,6) leads to the conclusion that the defect nature is the same for the two series (similar width of the bands, no significant shift of the defect bands toward the high wavenumbers).

Coals

Raman spectra have been recorded on vitrinite particles from coals of different ranks hence different reflectances (Figure 14). There are always two bands, one at about 1350 cm^{-1} and the other at about 1600 cm^{-1} shifted to the red in comparison with graphite. As noted by other authors (48), the half-maximum width of the last band (l_{1600}) decreases when the rank i.e. the reflectance in oil (R) of the coal increases (Figure 15). This decrease is very sudden for $R \leq 1\%$, then slower for $1 < R \leq 2\%$ and nearly zero for $R > 2\%$. Moreover, we have shown that the specific surfaces of the 1350 cm^{-1} band, of the 1600 cm^{-1} band, and the ratio S_{1350}/S_{1600} remain constant whatever the studied coals, i.e. in the whole coalification range.

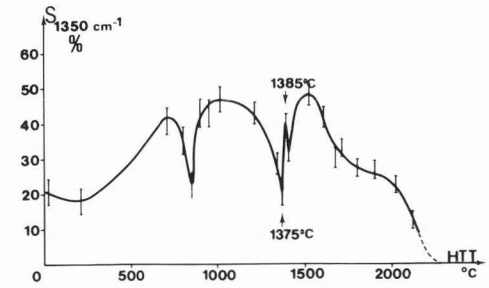

Figure 9 - S_{1350} versus HTT after decomposition of the spectrum in three bands (thick carbon films).

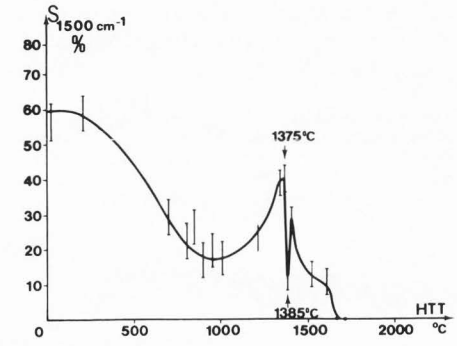

Figure 10 - S_{1500} versus HTT after decomposition of the spectrum in three bands (thick carbon films).

Discussion of Raman Results in Correlation with Electron and Optical Microscopy

The aim of the present work is to follow the evolution of the Raman spectra of homogeneous series of carbons obtained each from heat-treatment of a different precursor. Most authors, except Lespade (20), have rather described the spectrum modifications of different carbonaceous material types (pyrocarbons, various cokes, ground graphite, carbon fibers, etc). They have only related the observed decrease of the defect band to the aromatic layer diameter L_a (25).

Here, we can correlate the Raman data with those obtained by optical and electron microscopy in order to confirm and explain the ones by the others.

The optical and electron microscopy data are detailed in the Rouzaud thesis (39).

Optical microscopy data, obtained on bulk materials, show that optical parameters such as the reflectance and the extinction coefficient (calculated refractive indexes increase too, but the precision with which they are obtained is low) increase linearly with the temperature of treatment and with the hydrogen to carbon atomic ratio until a plateau is reached near 900-1000°C for all materials. Then, the optical parameters remain approximately constant until 3000°C. The level of this plateau depends on the microtexture of the carbon , i.e. the chemical composition of the precursor (oxygen to hydrogen

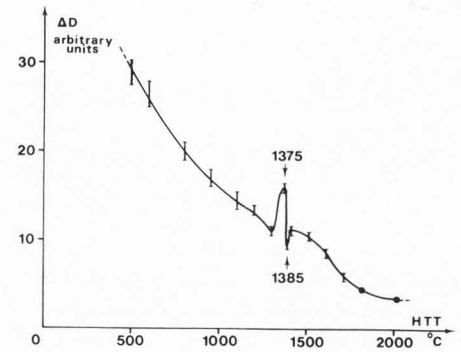

Figure 11 - Variation ΔD in the 002 interfringe spacing versus HTT (thick carbon films).

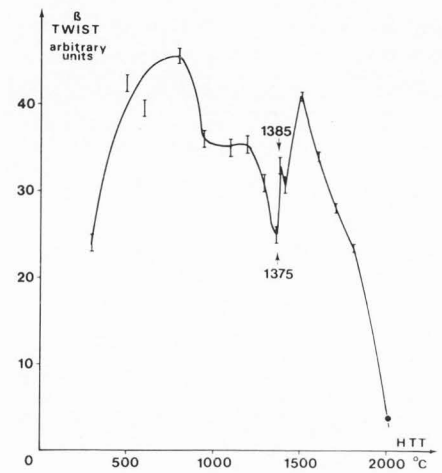

Figure 12 - Twist angle ß versus HTT (thick carbon films).

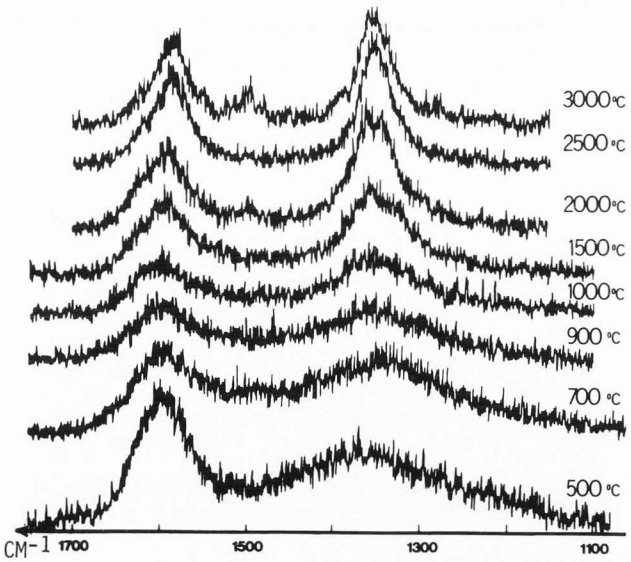

Figure 13 - Raman spectra of saccharose-cokes at different temperatures.

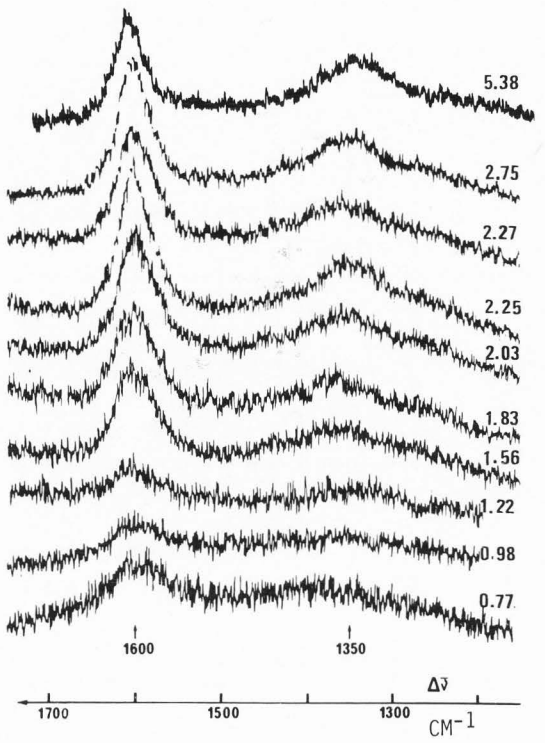

Figure 14 - Raman spectra of coals of different ranks. Corresponding vitrinite reflectance in oil is indicated above each spectra.

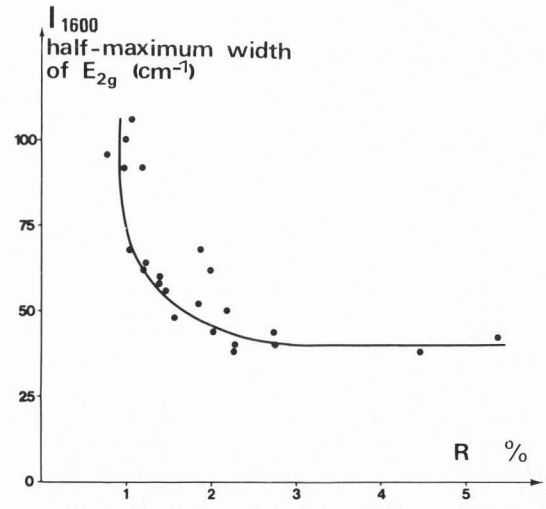

Figure 15 - Half-maximum width of the E_{2g} band versus vitrinite reflectance measured in oil (R).

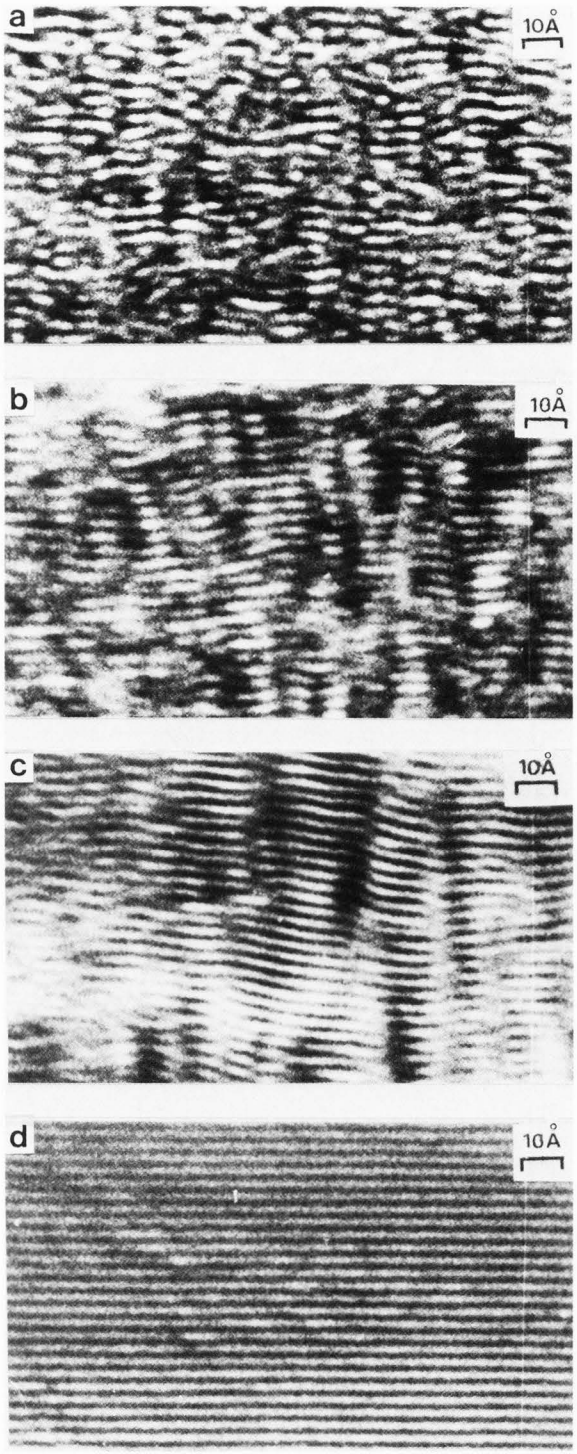

Figure 16 - Progressive graphitization (002 lattice fringes images) showing the increase in the number of parallel layers in a stack and progressive occurrence of perfect aromatic layers as HTT increases (anthracene-cokes).
a: 800°C; b: 1300°C; c: 1600°C; d: 2100°C.

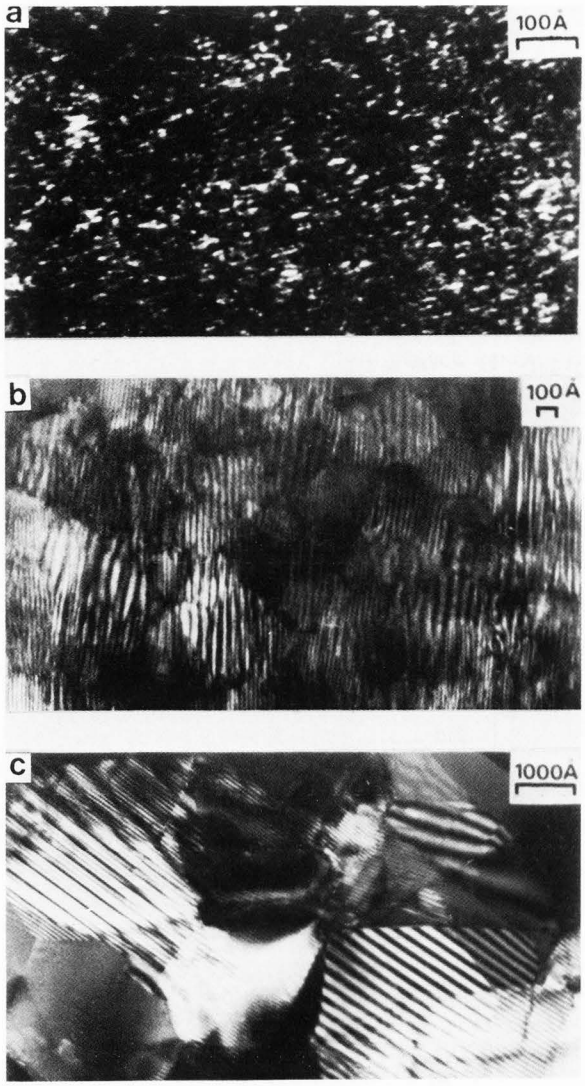

Figure 17 - Growth of the layer diameter L_a (11 dark-field images) (anthracene-cokes).
a: 1600°C; b: 2100°C; c: 2500°C.

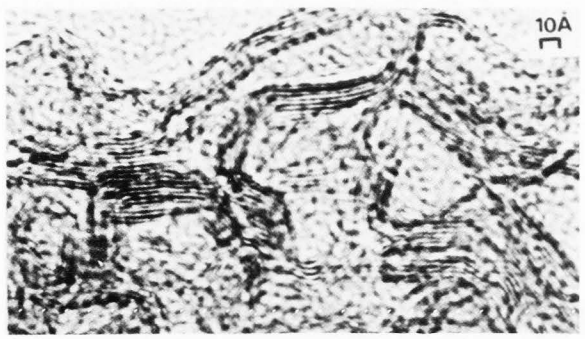

Figure 18 - 002 lattice fringe image showing porous microtexture in saccharose-coke heat-treated at 2800°C.

atomic ratio) (39). Oxygen-poor precursors (anthracene, for instance) are graphitizable and the level of the plateau is that of graphite. Oxygen-rich precursors (saccharose, for example) are not graphitizable and remain biperiodic even at 3000°C; their plateau is much lower than the corresponding graphite values. Intermediate materials such as cokes issued from heat-treatment of coals have plateaus between the saccharose and graphite values.

Figures 16 and 17 summarize the observations made by electron microscopy throughout the heat-treatment for anthracene-cokes. For the other graphitizable series, the evolution is nearly the same. However the improvement of graphitization necessitates temperatures which may vary according to the precursor.

This evolution of anthracene-cokes from 450 to 2900°C can be decomposed in successive steps during which the BSUs rearrange themselves progressively for obtaining large planar layers. The BSUs are constituted with polyaromatic structures less than 12 rings in diameter either single or stacked in parallel in twos or threes. At first, they are isolated for the most part (Figures 16a and 17a). Until 800°C, hydrogen is released but the size of BSUs remains constant. The number of isolated BSUs begins to decrease since they aim to join facing together in order to pack into distorted columns. Then, from 800°C, the distorted columns develop in the whole sample. The number of isolated and misoriented BSUs decreases gradually (Figure 16b) and becomes zero at 1500°C. Above 1500°C, the aromatic layers of two adjacent columns are facing and coalesce by forming distorted layers with a characteristic zigzag texture (Figure 16c). The thickness N of the stacks increases. From 1700°C, the distorted layers exist always, however they have progressively larger radii of curvature. The diameter L_a increases slowly until 1900°C. Between 1900 and 2100°C, the SAED patterns show the improvement of the graphite order (tridimensional) instead of the turbostratic order (bidimensional), formation of small crystallites occurs (Figure 17b). At 2100°C (Figure 16d), the aromatic layers are stiff and equidistant (β=0, ΔD = 0). The triperiodic order develops and the size of crystallites increases rapidly (Figure 17c).

The saccharose-cokes (non-graphitizable materials) have the same microtextural steps as the anthracene-cokes. However, the molecular orientation is limited to 100 Å because of the reticulation of the material by its oxygen. So, the increase of the stiff layer diameter is limited to a wall of pore (Figure 18) (corresponding to a molecular orientation); this prevents the development of the triperiodic order and the crystalline growth.

The parameters which permit to compare the results obtained by Raman microspectroscopy and electron microscopy, are the diameter L_a and the specific surface of the Raman band at about 1350 cm^{-1}. The values of L_a are directly measured from lattice fringes and 11 dark-field micrographs where crystallites are directly imaged. These L_a values somewhat differ from the mean values deduced from the X-Ray diffraction patterns used

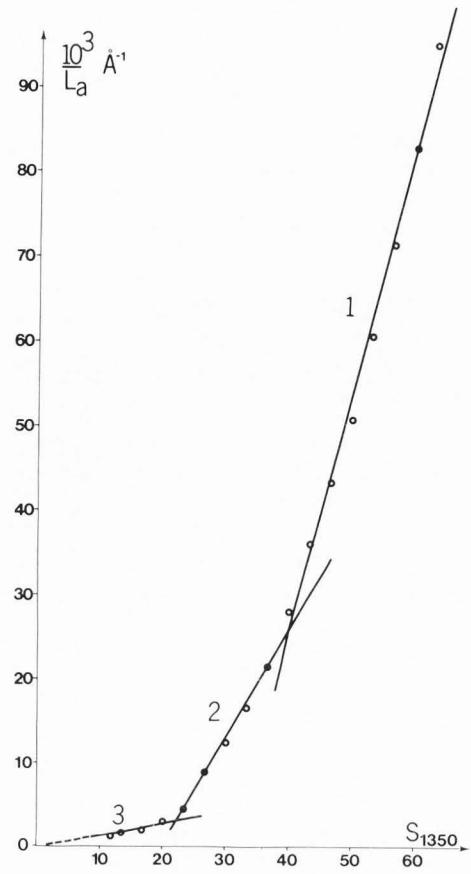

Figure 19 - $10^3/L_a$ versus S_{1350} (anthracene-cokes).

by Nakamizo (25). When $10^3/L_a$ is plotted versus S_{1350}, we obtain three well-defined straight lines (Figure 19-21). The slopes of these straight lines depend on the reference graphitizable carbon series.

In the case of anthracene-cokes (Figure 19), the following assumption can be made. The first straight line segment, corresponding to the room temperature-1600°C range, is attributed to the release of defects out of the average plane of the aromatic layers i.e. heteroatoms then isolated and misoriented BSUs of which the weak decrease of the number leads to a weak increase of L_a (10 to 35 Å) and the formation of distorted columns. The second straight line, corresponding to the 1600-2000°C range, is attributed to the removal of the defects in the average plane of the aromatic layers at zigzag level, which permits a moderate L_a increase (35 to 250 Å) and the formation of stiff and perfect layers. The third straight line, corresponding to temperatures above 2000°C, is attributed to the removing of grain joints or defects between two regions of stiff layers, leading to a very rapid increasing of L_a up to values greater than the diameter of the field of view of the microscope, justifying the extrapolation of the last straight line to zero (the crystallites seem infinite by comparison to

the probe size). The degree of graphitization increases and the tridimensional order is progressively set up during this last stage.

For the carbon film series (Figures 20 and 21), the curves $10^3/L_a$ versus S_{1350} are also formed with three straight segments, the slopes of which are different between them and from those of anthracene-cokes. These three slopes can be related to the types of defects present and their ease of removal. In the range corresponding to the second straight line, L_a increases more rapidly in the carbon films than in the anthracene-cokes whereas the same amount of defects is eliminated. That is probably due to the fact that one supplementary type of defect only in the carbon films hinders the L_a increase until enough energy is given to the system to release it. But, as soon as this type of defect -which can be tetrahedral carbons- is removed, the L_a can increase rapidly. For the saccharose-cokes, the correlation between L_a and S_{1350} does not permit to produce useful information because the defects are always abundant and the grain joints replace the other defects above 2000°C. L_a is not over 100 Å. So, S_{1350} does not vary significantly during heat-treatment.

Other information on the successive removal of different types of defects can be deduced from half-maximum widths (l_{1580} and l_{1350}) and the frequency of the Raman bands related to the microscopy observations. l_{1580} is much more important for the carbon films than for the anthracene-cokes (Figure 5). This, together with a marked frequency shift of the defect bands, only visible in the carbon films (Figure 6b) suggests again that these last materials contain a supplementary specific type of defect, such as tetrahedral carbon between BSUs. Their sudden release, before 1400°C provokes oscillation phenomena in the microtexture of the films (cf. variations of ΔD and β, Figures 11 and 12), responsible for similar oscillation phenomena in the 1350 and 1500 cm^{-1} Raman defect bands.

From room temperature to 1500°C, l_{1580} is roughly the same for the carbons issued from both the anthracene and saccharose semi-cokes. Moreover, the wavenumber of their defect band remains close to 1350 cm^{-1}. This suggests that they must contain the same type of bond.

The fact that the l_{1580} remains nearly constant in the saccharose-cokes and the defect band does not disappear confirms that the defects remain always abundant preventing the crystal growth, whereas the defect band disappears completely for the other series, expressing the elimination of all defects and the crystal growth.

With regard to the coals, the parameters used to compare the Raman and microscopy results are the l_{1600} and the reflectance in oil (R) of the vitrinite of the coals (Figure 15) correlated with elemental analysis. The decrease of l_{1600} with the degree of coalification (rank), for instance expressed by R, is attributed to the differential enrichment of the coal in polyaromatic structural units. This is due to progressive elimination of different chemical functions as demonstrated by elemental analyses (10,11,39) and infrared spectroscopy (10,36-38). At first ($R \leqslant 1\%$), oxygenated functions are released as H_2O and CO_2, then hydrogenated functions first ($1 < R \leqslant 2\%$) as liquid hydrocarbons and then ($R > 2\%$) as gaseous ones.

Moreover, the specific surface S_{1350} remains nearly constant showing that there is no crystalline

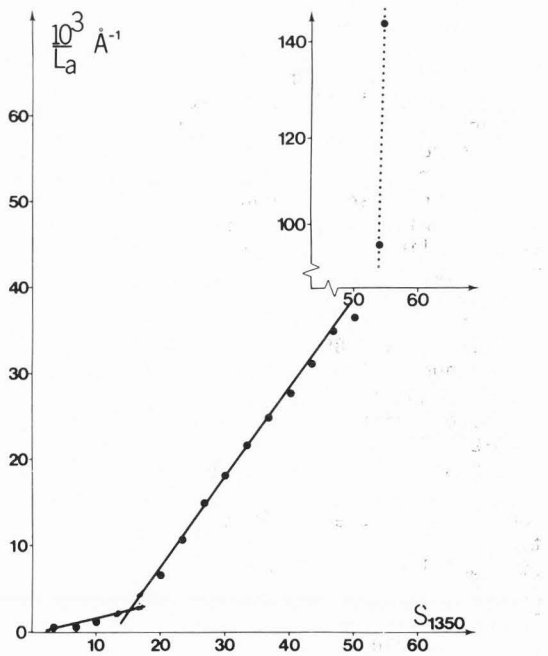

Figure 20 - $10^3/L_a$ versus S_{1350} (thick carbon films).

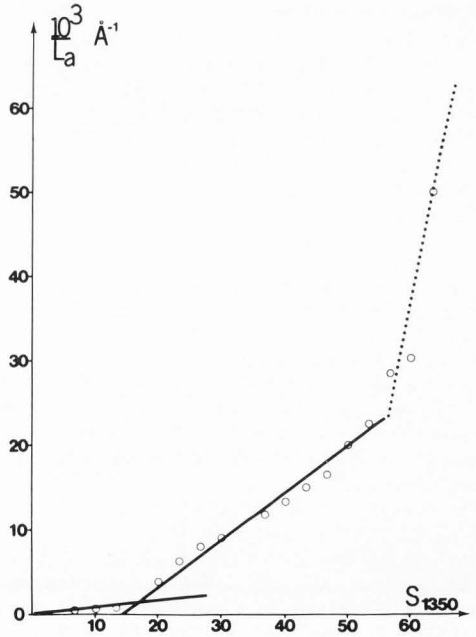

Figure 21 - $10^3/L_a$ versus S_{1350} (thin carbon films).

growth in the coalification range. The same conclusion has been deduced from electron microscopy data. Finally, the ratio S_{1350}/S_{1600} remains also constant, probably because S_{1600} increases with the enrichment in polyaromatic structural units and simultaneously S_{1350} increases also by the occurrence of defects out- and in- plane or aromatic layers related to the development of local molecular orientations ($\sim$ 100 Å in size) for R$\sim$2%, then of a statistical molecular orientation for high rank coals (anthracite stage) (3,4,40).

Conclusion

The comparison between elemental analysis, electron microscopy, optical microscopy and Raman microspectroscopy, performed on four reference carbon series realized by heat-treatment from four precursors (anthracene, thin and thick carbon films and saccharose), has permitted us to establish a model of carbonization and graphitization processes. This model serves as a basis for interpreting the coalification process and also the graphitization of other carbonaceous materials such as coals.

Therefore, the evolution of carbonaceous materials, throughout natural coalification and/or artificial (carbonization, graphitization) heat-treatment, is due to the elimination more or less rapid and more or less complete of different types of defects permitting the progressive rearrangement of the BSUs.

With the help of Raman microspectroscopy, it is possible to evidence different types of defects and to follow their variations during the evolution of the materials. Electron microscopy permits the direct imaging of planar polyaromatic structures, their arrangement in space (microtexture) and to follow crystal growth and triperiodic order improvement. The coupling of Raman microspectroscopy with high resolution electron microscopy, appears very powerful for a fine characterization of carbon materials.

All studies performed to date will allow us to begin work on various carbonaceous materials such as cokes from coals or carbonaceous particles included in minerals, for example.

Acknowlegments

We gratefully acknowledge Pr. M. Delhaye for the facilities in the use of the M.O.L.E. in LASIR (Lille, France). Samples of coals and their optical analyses have been kindly furnished by I.F.P. (Institut Français du Pétrole; Rueil-Malmaison, France) and CERCHAR (Centre de Recherches des Charbonages de France; Marienau, France).

References

1. Alpern B. (1969). Le pouvoir réflecteur des charbons français. Applications et répercussions sur la théorie de A. Duparque, (Reflectance of French coals. Applications and repercussions on A. Duparke's theory). Ann. Soc. Geol. Nord, 89, 143-166.
2. Alpern B, Bouroz A, Delattre Ch, Dolle P, Meriaux E, Noel R, Quinot E. (1970). Pétrologie des charbons, (Coal petrology). Ann. Soc. Geol. Nord, XC, 4, 203-222.
3. Bény-Bassez C, Rouzaud JN, Oberlin A. (1981). Premières applications de la microsonde MOLE à effet Raman à l'étude d'une série de charbons, (First applications of MOLE Raman microprobe to the study of a series of coals). C.R. Acad. Sci. Paris, 293, Ser. II, 509-512.
4. Bonijoly M, Oberlin M, Oberlin A. (1982). A possible mechanism for natural graphite formation. Intern. J. Coal Geol., 1, 283-312.
5. Boulmier JL, Oberlin A, Rouzaud JN, Villey M. (1982). Natural organic matters and carbonaceous materials: a preferential field of application for transmission electron microscopy. Scanning Electron Microsc. 1982; IV: 1523-1538.
6. De Fonton S, Oberlin A, Inagaki M. (1980). Characterization by electron microscopy of carbon phases in hard carbons when heat-treated under pressure. J. Materials Science, 15, 909-917.
7. Delhaye M, Dhamelincourt P. (1975). Raman microprobe and microscope with laser excitation. J. Raman Spectrosc., 3, 33-43.
8. Delhaye M, Bridoux M, Dhamelincourt P, Barbillat J, Da Silva E, Roussel B. (1982). A new generation of laser microspectrometers: Micromars. In: Microbeam Analysis, Heinrich KFJ.(ed) San Francisco Press, 275-278.
9. Dhamelincourt P. (1979). Developments and applications of the MOLE laser Raman microprobe. In: Microbeam Analysis, Newbury DE. (ed.) San Francisco Press, 155-164.
10. Durand B, Nicaise G, Roucaché J, Vandenbroucke M, Hagemann HW. (1975). Etudes géochimiques d'une série de charbons, (Geochemical studies of a series of coals). In: Adv. Org. Geochem., Campos R, Goni J. (eds), Enadimsa, Madrid, Spain, 1977, 601-631.
11. Durand B, Monin JC. (1980). Elemental analysis of kerogens. In: Kerogen, Durand B. (ed.), Technip, Paris, 113-142.
12. Ergun S. (1968). X-Ray studies of coals and carbonaceous materials. U.S. Dept. Int. Bureau of Mines, 648, 1-35.
13. Ergun S. (1968). Optical studies of carbons. In: Chemistry and Physics of Carbon, Walker PL. (ed.) Marcel Dekker, N.Y. 3, 45-119.
14. Franklin RE. (1950). The interpretation of diffuse X-Ray diagrams of Carbon. Acta Cryst., 3, 107-121.
15. Franklin RE.(1951). Croissance des cristallites dans les carbones graphitables et non-graphitables, (Growth of crystallites in graphitizable and non-graphitizable carbons). Proceed. Royal Soc., 209, 196-218.
16. Garza-Gomez A. (1982). La pétrographie des textures optiques des cokes et ses applications, (Petrography of optical textures of cokes and its applications). Thesis Dr. Ing., Univ. Orleans.
17. Goma J, Oberlin M. (1980). Graphitization of thin carbon films. Thin Solid Films, 65, 221-232.
18. Joseph D, Oberlin A. (1983). Oxidation of carbonaceous matter. Part 1: elemental analysis (C, H, O) and infrared spectroscopy. Carbon, 21, 559-564.
19. Lespade P, Marchand A, Merle AM, Pacault A. (1981). Méthodes nouvelles de caractérisation des

carbones, (New methods of characterization of carbons). Rev. Chim. Minérale, 18, 509-519.
20. Lespade P. (1982). Contribution à l'étude de la graphitation des carbones par microspectroscopie Raman. Application aux matériaux composites carbone-carbone, (Contribution to the study of the graphitization of carbons by Raman microspectroscopy. Application to carbon-carbon composite materials). Thesis Dr. Ing., Univ. Bordeaux.
21. Mac Cartney JT, Ergun S. (1967). Optical properties of coals and graphite. U.S. Dept. Int. Bureau of Mines, 641, 1-49.
22. Mering J, Maire J. (1965). Aspects structuraux de la graphitisation, (Structural aspects of graphitization). In: Les Carbones, Pacault A. (ed.) Masson, Paris,1, 129-192.
23. Milanovitch FP, Hirschfeld T, Johnson DC. (1982). The Lawrence Livermore National Laboratory Raman Microprobe, In: Microbeam Analysis, Heinrich KFJ. (ed.) San Francisco Press, 270-274.
24. Monthioux M, Oberlin M, Oberlin A, Bourrat X, Boulet R. (1982). Heavy petroleum products: microtexture and ability to graphitize. Carbon, 20, 167-176.
25. Nakamizo M, Kammereck R, Walker PL Jr. (1974). Laser Raman studies on carbons. Carbon, 12, 259-267.
26. Nemanich RJ, Solin SA. (1979). First- and second-order Raman scattering from finite-size crystals of graphite. Phys. Rev. B, 20, 392-401.
27. Oberlin A. (1979). Application of dark-field electron microscopy to carbon study. Carbon, 17, 7-20.
28. Oberlin A. (1982). Microtexture et propriétés des matières carbonées, (Microtexture and properties of carbonaceous matters). J. Microsc. Spectrosc. Electron, 7, 327-340.
29. Oberlin A, Boulmier JL, Durand B. (1974). Electron microscope investigation of the structure of naturally and artificially metamorphosed kerogens. Geochim. Cosmochim. Acta, 38, 647-650.
30. Oberlin A, Terriere G. (1973). Etude de la graphitation d'un carbone d'anthracène, (Graphitization of an ex-anthracene-carbon). J. Microscopie, 18, 247-252.
31. Oberlin A, Terriere G. (1975). Graphitization studies of anthracites by high resolution electron microscopy. Carbon, 13, 367-376.
32. Oberlin A, Terriere G, Boulmier JL. (1975). Carbonification, carbonization and graphitization as studied by high resolution electron microscopy. Tanso, Part I, 80, 29-42.
33. Oberlin A, Terriere G, Boulmier JL. (1975). Carbonification, carbonization and graphitization as studied by high resolution electron microscopy, Tanso, Part II, 83, 153-170.
34. Oberlin A, Villey M, Combaz A. (1980). Influence of elemental composition on carbonization. Carbon, 18, 347-353.
35. Robert P. (1971). Etude pétrographique des matières organiques insolubles par la mesure de leur pouvoir réflecteur. Contribution à l'exploration pétrolière et à la connaissance des bassins sédimentaires, (Petrographic study of insoluble organic matters by measuring their reflectance. Contribution to oil exploration and to the knowledge of sedimentary basins). Rev. Inst. Franç. Pétr., 24, 105-136.
36. Rouxhet PG, Robin PL. (1978). Infrared study of the evolution of kerogens of different origins during catagenesis and pyrolysis. Fuel, 57, 533-540.
37. Rouxhet PG, Villey M, Oberlin A. (1979). Infrared study of the pyrolysis products of sporopollenin and lignite. Géochim. Cosmochim. Acta, 43, 1705-1713.
38. Rouxhet PG, Robin PL, Nicaise G. (1980). Characterization of kerogens and of their evolution by infrared spectroscopy. In: Kerogens, Durand B. (ed.) Technip, Paris, 163-190.
39. Rouzaud JN. (1984). Relations entre la microtexture et les propriétés des carbones; application à la caractérisation des charbons, (Relationship between microtexture and properties of carbons; application to coal characterization). Thesis Dr. ès Sc., Univ. Orléans.
40. Rouzaud JN, Oberlin A. (1981). Structural and microtextural studies of natural and heat-treated coals. In: Proc. Intern. Conf. Coal Sci., Düsseldorf, Verlag Glückauf GmbH, Essen, Germany, 663-668.
41. Rouzaud JN, Oberlin A, Bény-Bassez C. (1983). Carbon films: structure and microtexture (optical and electron microscopy, Raman spectroscopy). Thin Solid Films, 105, 75-96.
42. Steinbach WR, Lohrstorfer CF, Etz ES. (1982). Analytical applications of a multiplex detector laser Raman microprobe. In: Microbeam Analysis, Heinrich KFJ. (ed.) San Francisco Press, 279-285.
43. Teichmüller M. Teichmüller R. (1979). Diagenesis of coal. In: Diagenesis in Sediments and Sedimentary Rocks, Larsen G, Chilingar GV. (eds.) Elsevier, Amsterdam, 25A, 207-246.
44. Tuinstra F, Koenig JL. (1976). Raman spectrum of graphite. J. Chem. Phys., 53, 1126-1130.
45. Van Krevelen DW. (1961). Coal chemistry, the main chemical reaction processes of coal. In: Coal, Elsevier, Amsterdam, 155-304.
46. Van Krevelen DW. (1961). The spatial structure of the coal molecules. In: Coal, Elsevier, Amsterdam, 312-342.
47. Vidano R, Fischbach DB. (1978). New lines in the Raman spectra of carbons and graphite. J. Am. Ceramic Soc., 61, 13-17.
48. Zerda TW, John A, Chmura K. (1981). Raman studies of coals. Fuel, 60, 375-378.

Discussion with Reviewers

F. Adar: All of the Raman work reported here was performed on the MOLE. However, the microscopic capabilities have not been exploited in this work. A comment regarding the potential of a Raman microprobe in differentiating various regions of a heterogeneous sample would be useful.

Authors: We have used the MOLE (Molecular Optical Laser Examiner) to observe and analyze the samples at the scale used for reflectance measurements. Moreover, for carbon films, optical microscopy is necessary to localize non-folded areas and, for coals, to diagnose vitrinite. On the other hand, the samples -as well carbon films as coal vitrinite- are in too small areas (100 to a few 1000 μm^2) to be localized and analyzed without a microscope. Actually, if the different phases of

a heterogeneous material are structurally different, their Raman spectra can be distinguished (20). However it is not possible to realize "maps" giving the distribution of the various carbonaceous phases in a heterogeneous sample, because the involved Raman bands are broad and the frequency shifts relatively small. Therefore the most important data obtained from Raman spectra concern the relative intensities of the two bands and their widths.

E.S. Etz: In the case of the Raman microanalysis of polished sections of carbonaceous materials (e.g., cokes and coals), it has been estimated that the depth of probing (skin depth) into the specimen surface may be no more than a few hundred angströms. Thus all the structural information derives from the first few layers of the surface.

What is the effect of polishing on the microstructure and topography of the specimen surface and subsurface?

Authors: The probing depth does not appear negligible to us because Lespade's work (20) on carbonaceous material indicates a depth of about 1000Å which agrees with the data of Vidano (47). This corresponds to about 300 piled up aromatic layers. In the case of carbon films, the probing depth is thus larger than the thickness of films so that information concerns the whole material. Electron microscopy studies show that both carbon films and anthracene-cokes are graphitizable and that graphitization follows the same stages. For Raman spectroscopy no specific preparation was made for carbon films, whereas anthracene-cokes were polished. Raman spectra were recorded in the same conditions on areas where the aromatic layers are perpendicular to the laser beam (such areas being dark between crossed polarizers). The obtained Raman spectra show the same stages of graphitization for both materials, the small differences between them being also detected through electron microscopy. Moreover the spectra we obtained on anthracene-cokes and saccharose-cokes agree respectively with those performed by Lespade (20) on pellets of these materials dispersed in a matrix of pressed solid potassium bromide. Consequently the polishing such as it has been carried out (39) has no effect on the Raman data.

E.S. Etz: Other workers [R.P. Vidano et al., Solid State Communications, Vol. 39, pp. 341-344 (1981) and Mernagh et al. (52)] have reported bands in the Raman spectra of carbons at frequency shifts other than 1350 and 1600 cm^{-1}.

These new carbon bands have been reported at about 1470 cm^{-1}, 2700 cm^{-1} and 2950 cm^{-1} and have tentatively been attributed to either functional groups such as C=O vibrations of surface oxidized species, C-H stretching, or non-fundamentals. Have these or similar bands also been observed in the spectra of the carbonaceous materials studied here?

Authors: The Raman spectra have been recorded only in the 1000-1800 cm^{-1} range and in the conditions chosen above (avoiding degradation). They show usually broad defect band. For thick carbon films, the spectra have been decomposed into three bands at about 1350, 1500 and 1580 cm^{-1}. The second one is placed at a frequency close to the 1470 cm^{-1} band described by Mernagh who has attributed it to C=O band (52). Such a hypothesis cannot be retained for thick carbon films which are pure carbons. We have demonstrated the band at about 1500 cm^{-1} is due to structural defects (41). Cokes heat-treated up to 1000°C being also practically pure carbons cannot give bands due to chemical functions. It is only for cokes heat-treated below 1000°C and for coals that oxygenated and hydrogenated functions could exist. However their spectra have a shape similar to that of pure carbons having an identical structural organization. It seems better to use infrared spectroscopy for trying to set into evidence possible oxygenated functions because they give rise to bands more intense than in Raman spectroscopy.

J. Minkin: For what other carbonaceous materials do you think studies of this type might be of particular value?

Authors: Studies of this type (combined use of Raman microspectrometry, electronic and optical microscopy) may be of particular value for:
- heterogeneous materials at the scale of optical microscope, such as carbon-carbon composites (20), various components of natural organic matters (coal macerals);
- homogeneous series e.g. series of parent-rocks of oil sampled along a bore-hole, series of partially graphitizable materials heat-treated from room temperature up to 3000°C;
- materials which can be studied only in situ such as carbon present in fluid inclusions.

J. Minkin: Have you done any studies on individual vitrinite samples over the same range of temperatures used with your reference carbon series? If so, do these results differ from the results obtained at room temperature with samples over the range of reflectance values, and can you interpret the source of such differences? Could such a set of data be obtained also on a single vitrinite sample over a range of increasing pressures to evaluate the importance of such parameters in the coalification process?

Authors: We have not yet studied vitrinites heat-treated between room temperature and 3000°C by Raman microspectrometry. However studies are carried out on coals, pyrolyzed at 1000°C, by electron and optical microscopy. The first data are given in the Rouzaud thesis (39). Complete results will be soon submitted to Fuel. They show that at about 500°C, the structural units of coals locally orient parallel, to form local molecular orientations (LMO). Their extents depend on the value of the O/H ratio at the moment the molecular orientation settles (40,53). Hence, according to the coal, the LMO size after pyrolysis varies between that of saccharose-cokes ($\leq$ 100 Å) up to that of anthracene-cokes ($\gg 1\mu m$) (53). On the other hand raw coals, even of high rank, have only LMO of small extent ($\leq$ 100 Å). The LMO size has been shown to depend on the manner the oxygenated and/or hydrogenated functional groups depart from the precursor

(24,39,49,50). Consequently it is necessarily different for pyrolyzed coals and for coals submitted only to the geothermal gradient, their respective heating rates being very different. Concerning optical microscopy, reflectance increases with temperature, thus with the departure of oxygenated and hydrogenated groups. It reaches a maximum at about 800-1000°C. The value of this maximum is placed between the value of the anthracene-coke plateau and the value of the saccharose-coke plateau. The larger the size of the coke LMO, the higher the value. Thus there are as many reflectance increase laws as there are coals. Hence raw or pyrolyzed coals, chemically and/or microtexturally different, may have a same reflectance.

Concerning the pressure parameter, no study has been performed either by Raman spectroscopy or by optical microscopy. Yet it has been shown by electron microscopy that carbons which are non-graphitizable under the effect of temperature alone, become graphitizable when moreover submitted to pressure (4,6,31). Graphitization then occurs by phase changes at temperatures lower than those requested for the progressive graphitization of anthracene-cokes. Thus saccharose-cokes pyrolyzed at 5 kbar suddenly transform into graphite at ca. 1700°C (6). Presently we have not checked whether these two modes of graphitization could be differentiated by Raman microspectrometry and optical microscopy.

J. Minkin: How was the thickness of the evaporated carbon films determined?
Authors: The thickness of carbon films was evaluated by two ways. First, it was determined by an interferometric method developed by the "Institut d'Optique" (Orsay, France). Secondly, it was deduced from Cosslett's charts giving the thickness of an evaporated carbon film versus its optical density (51). The data obtained by both methods are in good agreement.

Additional References

49. Bourrat X, Oberlin A, Escalier JC. (1984). Influence des hétéroatomes sur le comportement thermique de quelques asphaltes, (Influence of heteroatoms on the thermal behavior of some asphalts), C.R. Acad. Sci., Paris, 298, Sér. II, 695-698.
50. Bourrat X, Oberlin A, Escalier JC. (1984). Rôle de la vitesse de carbonisation sur l'aptitude à la graphitation, (Influence of the carbonization rate on the graphitization ability), C.R. Acad. Sci., Paris, 298, Sér. II, 787-790.
51. Cosslett A, Cosslett VE. (1957). The optical density and thickness of evaporated carbon films, Brit. J. Appl. Phys., 8, 374-376.
52. Mernagh TP, Cooney RP, Johnson RA. (1984). Raman spectra of graphon carbon black, Carbon, 22, 39-42.
53. Rouzaud JN, Bensaïd F, Oberlin A. (1983). Caractérisation des charbons et des cokes par microscopie électronique par transmission, (Characterization of coals and cokes by TEM), Entropie, 113-114, 33-42.